Korean J. Chem. Eng., 35(4), 900-908 (2018)
DOI: 10.1007/s11814-017-0341-5

pISSN: 0256-1115
eISSN: 1975-7220

Treatment of penicillin with supercritical water oxidation: Experimental study of combined ReaxFF molecular dynamics

Tengzhou Ma*, Tingting Hu*, Dandan Jiang*, Jinli Zhang*, Wei Li*, You Han*,**,†, and Banu Örmeci***,†**

*School of Chemical Engineering and Technology, Tianjin University, Tianjin 300072, China
**Tianjin Key Laboratory of Membrane Science and Desalination Technology, Tianjin University, Tianjin 300072, China
***Department of Civil and Environmental Engineering, Carleton University,
1125 Colonel by Drive, Ottawa, Ontario K1S5B6, Canada
(*Received 13 July 2017 • accepted 12 December 2017*)

Abstract−Supercritical water oxidation (SCWO) of penicillin (PCN) was investigated under different operating conditions. The chemical oxygen demand (COD) removal rate could reach 99.4% at 400 °C, 24 MPa, 1 min and oxidation coefficient (OC) of 2. Experimental results showed that COD removal had no significant dependence on temperature and pressure variations. By contrast, COD removal could be significantly promoted with OC increasing from 0 to 2.0, but the effect was negligible as the OC further increased; similarly, longer residence time than a definite value seemed to contribute little to COD removal. Initial and deeper degradation pathways of penicillin were proposed based on the reactive force field (ReaxFF) molecular dynamics (MD) simulations. By tracing the evolution of intermediates, the migration routes of S and N during the SCWO process were obtained with H_2S and NO_2 produced as the corresponding products. Simulation results showed that SCW and oxidant not only accelerated the degradation by producing highly reactive radicals or molecules, but also participated in reactions by serving as H and O sources. Moreover, catalysis of water clusters in C-heteroatom bond cleavage was also observed.

Keywords: Penicillin, Supercritical Water Oxidation, ReaxFF, Molecular Dynamics Simulation, Degradation Pathway

INTRODUCTION

The presence of antibiotics in the environment has been critically discussed in relation to bacterial resistance and several human illnesses [1,2]. Special attention has been given to the β-lactam antibiotics because of their wide use in the treatment of infectious diseases. An example is penicillin, a β-lactam antibiotic widely used against bacteria by destroying cell walls in bacterial organisms [3,4]. As a consequence of the poor efficiency of conventional technologies applied in wastewater treatment plants, penicillin has been detected in different water bodies [5]. Therefore, it is urgent to develop a simple and efficient treatment method to eliminate the β-lactam antibiotics from wastewater.

Over the past decades, various processes have been developed to address the problem of antibiotics in natural water and wastewater. For example, activated carbon adsorption has been investigated for the treatment of pharmaceutical wastewater [6]. However, the removal extent of β-lactam antibiotics is largely dependent on the kind of antibiotics, and the low hydrophobicity as well as negative charge often leads to a poor removal [7]. In recent years, physicochemical techniques, especially advanced oxidation processes (AOPs), have shown to be a promising solution for antibiotic pollutants [8,9]. AOPs are based on the formation of oxidative species [10], mainly the hydroxyl radical, which is able to degrade organic compounds with high reaction rates. AOPs can be classified into photochemical and non-photochemical processes. The photocatalysis with TiO_2 (UV/TiO_2) and the photo-Fenton reaction ($UV/H_2O_2/Fe^{2+}$) are widely studied among the photochemical processes. On the other hand, one of the promising non-photochemical processes is ultrasound (US), which is based on the cavitation phenomenon [8], then the degradation can be initiated by the interaction of high frequency ultrasound with aqueous media to produce OH radicals or via pyrolysis. Nevertheless, previous studies [11,12] have suggested that antimicrobial activity and mineralization of AOPs are strongly influenced by the water matrix characteristics as well as additives; thus, the requirements of operating conditions and pretreatment boost the cost of wastewater treatment.

Supercritical water oxidation (SCWO) has been proposed as a powerful and promising technology for complete destruction of aqueous waste streams and high-risk wastes, such as municipal sewage [13], dyehouse wastes [14] and flammable industrial wastes [15]. When the temperature and pressure reach the critical point (T_C=374 °C, P_C=22.1 MPa), water acts as a special solvent with high diffusivity and excellent transport properties. Moreover, due to the relatively low dielectric constant, SCW can become completely miscible with organic compounds, thus creating a homogeneous reaction media without mass-transfer limitations [16]. The use of oxidant could greatly promote the degradation, and the most commonly used oxidant in SCWO is H_2O_2, which is conducive to producing highly reactive OH radicals according to the reaction given below [17]:

$$H_2O_2 \rightarrow 2\bullet OH \quad (1)$$

†To whom correspondence should be addressed.
E-mail: yhan@tju.edu.cn, banuormeci@cunet.carleton.ca

In this way, organics could be destroyed in extremely short reaction time with mainly water and carbon dioxide produced, so compared with traditional oxidation methods such as incineration, SCWO is an environmentally benign and effective method. Another advantage for SCWO is that liquid wastes can be used as feedstock directly, thus avoiding the additional process expenditures resulted from feedstock drying, pretreatment, and component separation.

The reaction mechanism of SCWO is important for process design and industrialization of the antibiotic wastewater treatment. However, because of the severe conditions and rapid SCWO reactions, it is a great challenge for experimental scientists to disentangle the various fundamental reaction steps from the intermediate and final product distribution. From this perspective, with the aid of molecular simulation, researchers can effectively probe different proposed hypotheses to gain insight into the underlying mechanism of SCWO on the length and time scales that is not accessible in experiments. The static density functional theory (DFT)-based ab initio calculations focus primarily on ground-state energies of elementary steps to derive an understanding of the reaction paths as well as barriers of the reaction steps [18]. There are many molecular simulation studies on SCW systems available in the literature, such as SCWO of ethanol [19], formic acid [20] and glyceralde [21]. In recent years, the ReaxFF molecular dynamics simulation has been an attractive option due to the less time and computational cost compared to the ab initio MD simulations [22,23]. In addition, ReaxFF has demonstrated its ability to describe SCW systems in a number of studies [24-27].

Yabalak et al. [28] reported subcritical water oxidation of 6-aminopenicillanic acid and cloxacillin with the optimum experimental parameters determined by response surface methodology, which was quite encouraging. However, to the best of our knowledge, the supercritical water oxidation of penicillin together with the reaction mechanism has not been investigated yet. In this paper, we chose penicillin (PCN) as a model compound of β-lactam antibiotics to investigate the effect of operation parameters on PCN removal. After which we performed ReaxFF molecular dynamics simulation to gain a thorough reaction mechanism and clarify the roles of SCWO system. The experimental and simulation results were advantageous for further experimental and industrial applications based on SCW reaction media.

MATERIALS AND METHODS

1. Materials

The penicillin power (purity >98%) used in this study was obtained from Tianjin Runxiang Biological Technology Corporation. Hydrogen peroxide was purchased as the H_2O_2 30 wt% aqueous solution from Jiangtian Chemicals Corporation, and diluted to the desired concentrations with deionized water. Digestion solution for COD was obtained from Hach Company.

2. Experimental Apparatus and Methods

A schematic of the experimental apparatus is shown in Fig. 1. A batch cylinder autoclave with a capacity of 500 cm^3 was used as a pressurized reactor, which was made of NS336 corrosion resistant alloy. After loading penicillin power and H_2O_2 solution, deionized water was fed into the autoclave in the desired amounts according

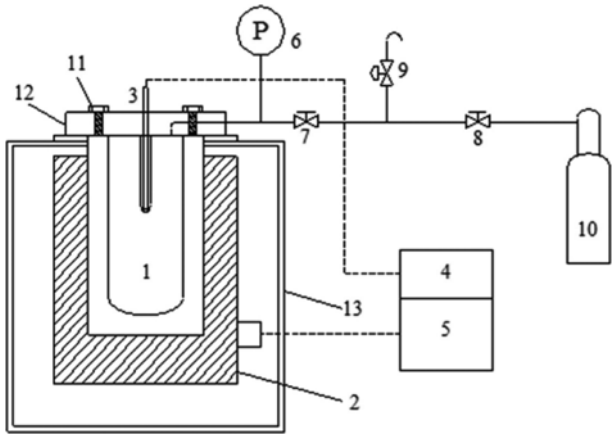

Fig. 1. Schematic diagram of experimental apparatus.

1. Reaction vessel	7, 8. Cut-off valves
2. Heating furnace	9. Air release valve
3. Thermal couple	10. N_2 high-pressure gas cylinder
4. Temperature indicator	11. Screws
5. Temperature indicator for heating furnace	12. Top cover
6. Pressure gauge	13. Support

to target temperature and pressure. The system was then sealed and purged with N_2 for three times to replace the residual air. After which the autoclave was heated by a temperature-controlled electric furnace to achieve the preset temperature and pressure. Temperature and pressure were measured by a K type thermocouple (with ±0.1 °C accuracy) and a pressure gauge (with ±0.1 MPa accuracy) during the heating process, respectively. After the desired reaction time had elapsed, the furnace was removed, and the autoclave was cooled by a fan. The liquid product was collected for further analysis. Ethanol was used to rinse the system before and after each experiment.

The digestion of liquid product was conducted in digestion instrument (HACH DRB200) for 120 mins. After digestion, the amount of chemical oxygen demand (COD) in the sample was measured by a commercial COD analyzer (HACH DR1010) based on Lambert-Beer law.

3. Data Interpretation

The oxidation coefficient (OC) and the COD removal rate are defined as Eqs. (2) and (3), respectively.

$$OC = \frac{[O_2]_{add}}{[O_2]_{need}} \tag{2}$$

where, $[O_2]_{add}$ is the oxygen (mg) formed from the decomposition of H_2O_2. $[O_2]_{need}$ is the stoichiometric oxygen (mg) needed to completely oxidize penicillin to CO_2, H_2O, SO_2 and NO_2.

$$\text{COD removal rate (\%)} = \left(1 - \frac{COD_{final}}{COD_{initial}}\right) \times 100\% \tag{3}$$

where, $COD_{initial}$ is initial COD content (mg L^{-1}) in the sample, COD_{final} is residual COD content (mg L^{-1}) in the liquid product.

In many studies, the COD removal rate is usually the main performance index for wastewater treatment techniques, while final concentration of COD is concerned to estimate whether the treated wastewater can meet related standards. Therefore, we also supplied

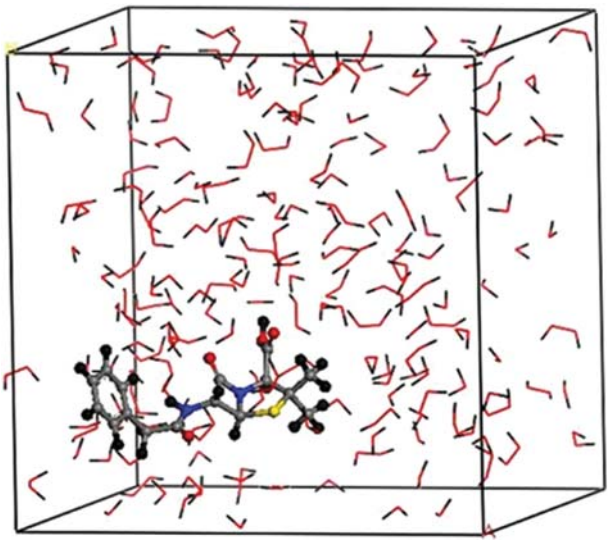

Fig. 2. The constructed simulation cell obtained by amorphous module using Material Studio.

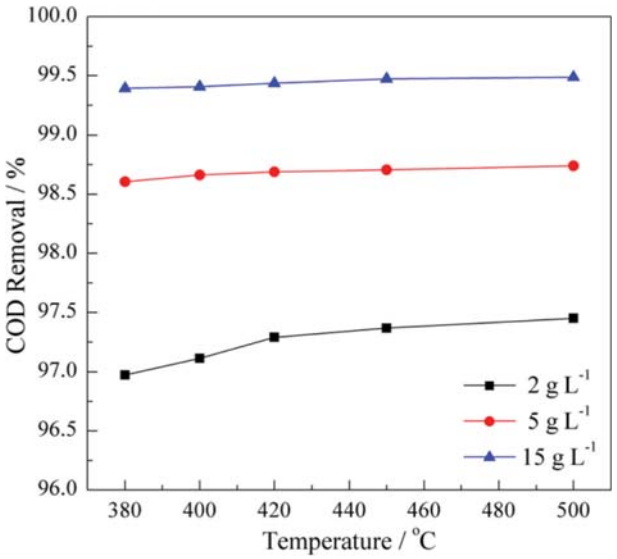

Fig. 3. Effect of temperature on COD removal (pressure: 24 MPa; residence time: 1 min; OC: 2).

the graphs based on the final concentration of COD in the Supporting Information (Fig. S1-Fig. S4).

4. The Method of Molecular Dynamics Simulation

In this work, we performed ReaxFF molecular dynamics (MD) simulations to investigate the degradation mechanism of PCN in SCWO system where H_2O_2 worked as the oxidant. The constructed simulation cell is shown in Fig. 2.

First, the molecular structures in a three-dimensional model were optimized using the Dmol^3 module, and the reaction models were constructed in periodic boxes using the amorphous cell module in Materials Studio software supplied by Accelrys Inc. The density functional theory (DFT) calculations are at the level of the generalized gradient approximation (GGA) with the Becke-Lee-Yan-Parr (BLYP) functional employed. The double-numerical plus polarization (DNP) basis set was also employed here, and the energy convergence criterion was set to be 0.00002 Hartree. Then, we used the Lammps software to carry out the ReaxFF MD simulations. Due to the limitation of computational simulation time, researchers always use a much higher temperature during the ReaxFF MD simulations instead of experimental temperature to investigate many reaction systems. For instance, Goddard et al. [29] tested the effect of the difference in temperature between simulation and experiment on the thermal decomposition of brown coal and concluded that it may certainly affect product distributions, but the reaction processes were not affected, Chen et al. [30] investigated lignite depolymerization in supercritical methanol with lignite-related model compounds via the ReaxFF MD simulations at a temperature as high as 2,200 K. Wang et al. [31] studied the thermodynamics of spinel surface deposition using the temperature range as 2,500-3,000 K. Our group also [24,25] studied the effect of supercritical water on coal pyrolysis and hydrogen production in a temperature as high as 2,400 K and investigated supercritical water oxidation and gasification for explosive wastewater treatment using the temperature range as 2,500-3,000 K. Thus, we selected a relatively high temperature of 2,500 K to reveal the mechanism of PCN degradation within a limited time scale. The time step was set as 0.1 fs and the NVT ensemble was applied for the simulations. A multi thermostat with a damping constant of 25 ps calculation was employed for the initial temperature from 2 to 300 K with a rising rate of 10 K ps^{-1}, then the system was equilibrated at 300 K. Next, the systems were heated to the reaction temperature with a rising rate of 100 K ps^{-1}. The reactive molecular dynamics simulations were carried out for 200 ps.

RESULTS AND DISCUSSION

1. Effect of Operation Parameters

1-1. Effect of Temperature on COD Removal

The effect of temperature on COD removal rate of three different initial PCN concentrations is illustrated in Fig. 3. After the treatment at 400 °C, COD removal rate of different initial PCN concentrations reached 97.1%, 98.2%, and 99.4%, respectively, indicating the great potential of SCWO used for PCN degradation. We predicted that, as the governing mechanism for SCWO was free radical [32], increasing temperature would promote the production of reactive radicals and increase the probability of collision between the radical species, thus accelerating the decomposition reaction. However, according to our experimental results, the removal rate of COD had no significant dependence on the temperature variations. Besides, reactants with higher initial PCN concentrations (5 g L^{-1} and 15 g L^{-1}) seemed less sensitive to temperature change. This could be explained by the decreasing concentration of reactants caused by the reduction of water density, consequently reduced the reaction rate. These two opposite effects arising from temperature made the removal of COD increase less significantly with the rising temperature. The result was in agreement with that of Wang et al. [33] about SCWO of coal. They observed the conversion of COD presented a nonlinear decreasing tendency towards temperature increment and ascribed this phenomenon to the formation of recalcitrant aromatic compounds. Considering the ben-

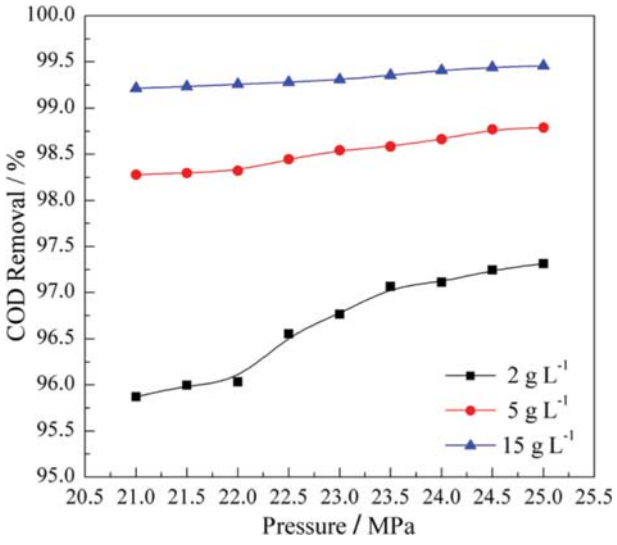

Fig. 4. Effect of pressure on COD removal (temperature: 400 °C; residence time: 1 min; OC: 2).

zene ring contained in PCN structure, the coupling of aromatic intermediates may be another reason for the unaffected COD removal rate.

1-2. Effect of Pressure on COD Removal

The effect of pressure on COD removal rate of three different initial PCN concentrations is illustrated in Fig. 4. Researchers have reported positive [34,35], insignificant [36,37] and even restraining effect [38] on SCWO process. As seen, similar to the effect of temperature, reactant with lower PCN concentration (2 g L^{-1}) was more sensitive to pressure, compared to those with higher PCN concentrations (5 g L^{-1} and 15 g L^{-1}). In our study, the effect of pressure on COD removal was not obvious, which may be for the following reasons: on the one hand, rising pressure accompanied with the increasing density of SCW system so as to the concentration of reactants; on the other hand, the cage effects [39] caused by SCW system would also increase with the pressure rising, which was unfavorable for the COD removal. Therefore, the combined effects diminished the overall effect of increasing pressure on the COD removal rate. In general, compared with other parameters, the effect of pressure was also found to be less significant in previous studies [33,40].

1-3. Effect of Oxidation Coefficient on COD Removal

The effect of oxidation coefficient (OC) on COD removal rate of three different initial PCN concentrations is illustrated in Fig. 5. In the range of OC<2, increasing OC significantly improved COD removal, with the further increase of OC; however, enhancement on COD removal was very limited. This phenomenon could be explained by free radical mechanism involved in SCWO reactions. As the concentration of H_2O_2 was increased, more OH radicals were generated to participate in PCN degradation and thus accelerated the decomposition. However, as the H_2O_2 concentration was considerably high, the OH radicals finally reached equilibrium with H_2O_2; in addition, less reactive species such as HO_2 radicals and O_2 were produced due to possible side reactions, which explained the reason for the stationary COD removal rate as the H_2O_2 concentration was further increased. Previous studies have reported some involved side reactions which were shown in Eqs. (4)-(7) [17,28]:

$$H_2O_2+\bullet OH \rightarrow HO_2\bullet+H_2O \quad (4)$$

$$H_2O_2+\bullet OH \rightarrow O_2^-\bullet+H^++H_2O \quad (5)$$

$$\bullet OH+\bullet OH \rightarrow H_2O_2 \quad (6)$$

$$\bullet OH+HO_2\bullet \rightarrow H_2O+O_2 \quad (7)$$

Therefore, there is an optimal value for OC to complete the degradation. Further increasing OC is meaningless expect for increasing the operating costs.

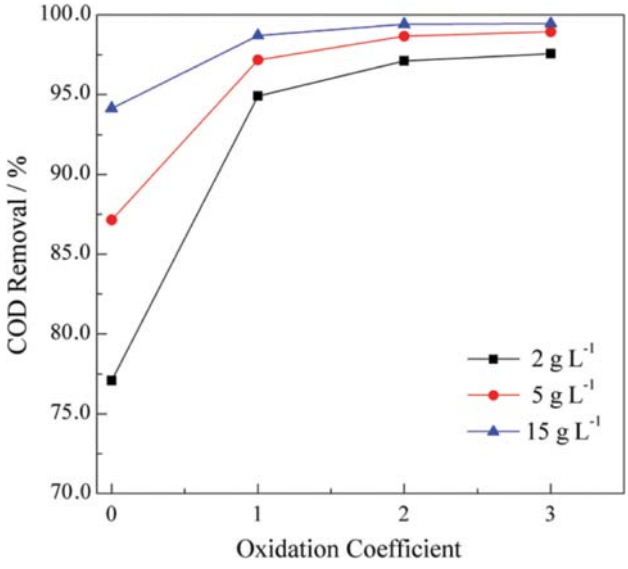

Fig. 5. Effect of oxidation coefficient on COD removal (temperature: 400 °C; pressure: 24 MPa; residence time: 1 min).

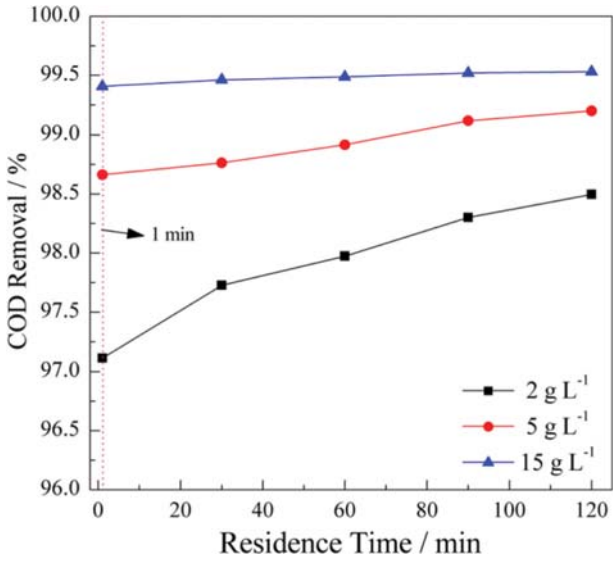

Fig. 6. Effect of residence time on COD removal (temperature: 400 °C; pressure: 24 MPa; OC: 2).

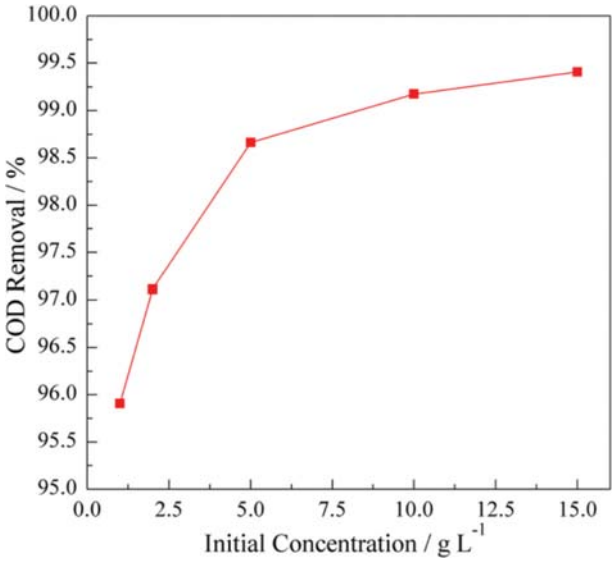

Fig. 7. Effect of initial PCN concentrations on COD removal (temperature: 400 °C; pressure: 24 MPa; residence time: 1 min; OC: 2).

1-4. Effect of Residence Time on COD Removal

The effect of residence time on COD removal rate of three different initial PCN concentrations is illustrated in Fig. 6. As can be seen, the effect of residence time on COD removal rate was very small when it exceeded a definite value. This phenomenon can be attributed to free radical reaction mechanism with initiation, propagation and termination steps involved [41]. Due to the rapid dissociation of H_2O_2 under SCW conditions, a critical concentration of radicals built up in initiation step in a short time, followed by attacks of these radicals in the propagation step. With the reaction time prolonged, termination reactions became dominant accompanied by the formation of refractory products, which hindered the further COD removal.

1-5. Effect of Initial PCN Concentrations on COD Removal

The effect of initial PCN concentrations on COD removal rate is illustrated in Fig. 7. As shown, COD removal rate became larger with an increase of initial PCN concentration; in fact, this trend was observed in the previous analysis. One possible explanation for this phenomenon is that higher initial concentrations would increase the probability of intermolecular collision, thus a better degradation was achieved. Besides, the relatively complex structure of PCN resulted in high steric hindrance, which was unfavorable to the degradation. Therefore, kinetics rather than thermodynamics significantly influenced the OH radicals attack. Thus the increase of intermolecular collision would promote the SCWO process from the viewpoint of kinetics.

2. ReaxFF Molecular Dynamics Simulation

A thorough reaction mechanism would not only be helpful for the application of SCWO technology in the field of PCN-containing wastewater treatment, but also help facilitate the conceptual design and analysis of chemical processes based on SCW reaction media. With the aid of molecular dynamics simulation based on ReaxFF force field, we could gain insight into the reaction pathways and product distribution. To be more specific, these simulation results would help to better explain the roles of SCW and oxidant during the degradation process, so as to optimize the process parameters for a better PCN removal.

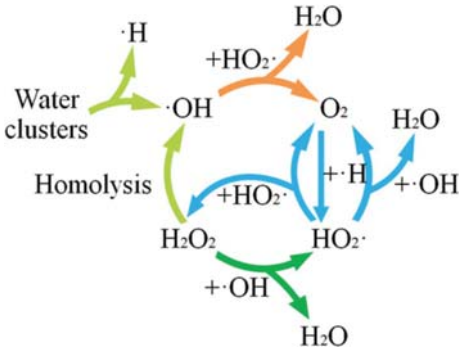

Fig. 8. The sources of active radicals during SCWO process.

2-1. The Sources of Active Radicals During SCWO Process

Water participates as a reactant in several elementary reaction steps that occur during SCWO, and the governing mechanism for SCWO is free radical [39]. Examples of such radical reactions, such as detailed chemical kinetics models for SCWO of phenol [34], benzene [42] and ethanol [43] were proposed previously. In this study, three types of radicals, namely, hydroxyl radical (•OH), hydrogen radical (•H), and peroxyl radical (HO_2•) were observed. The changes of water and hydrogen peroxide molecules were traced to elucidate the sources of radicals and O_2. The reaction paths among radicals in SCW are shown in Fig. 8.

There are mainly two ways for the production of OH radicals: One is from supercritical water, while the other one is from H_2O_2. The HO_2 radicals are mainly produced through H_2O_2 interacting with •OH and oxygen molecule interacting with •H, respectively. Meanwhile, O_2 are mainly produced through the interactions between HO_2• as well as HO_2• interacting with •OH. In fact, PCN can be attacked by five kinds of radicals or molecules including OH radical, HO_2 radical, O_2, H_2O_2, and H_2O, among which OH radical is the most effective oxidant during SCWO, which is consistent with the experimental studies of Savage et al. [44].

2-2. Initial Degradation of PCN During the SCWO Process

In this work, we analyzed the degradation mechanism of PCN in SCWO at the atomistic level. Making a comprehensive investigation on initial reaction mechanism is a prerequisite for subsequent analysis of key intermediates. By tracing the atoms in the simulation results, we obtained the possible initial reaction pathway of SCWO system as shown in Fig. 9.

Under the supercritical condition, the water molecules form clusters, such as dimers and trimers through hydrogen binding [45,46], which are beneficial for the degradation of PCN. The degradation of PCN consisted of the linear-chain cleavage and the opening reactions of two heterocycles and one aromatic ring. The heterocycles were opened first due to the structural instability of two neighboring heterocycles, and then the linear chain was broken. For example, the O4-H1 bond was broken via the attack of OH radical dissociated from water clusters. Then, O4 interacted with C12, which caused O4 to insert into the middle of C12 and C13. Subsequently, the C9-C10 bond and C11-S bond in the heterocy-

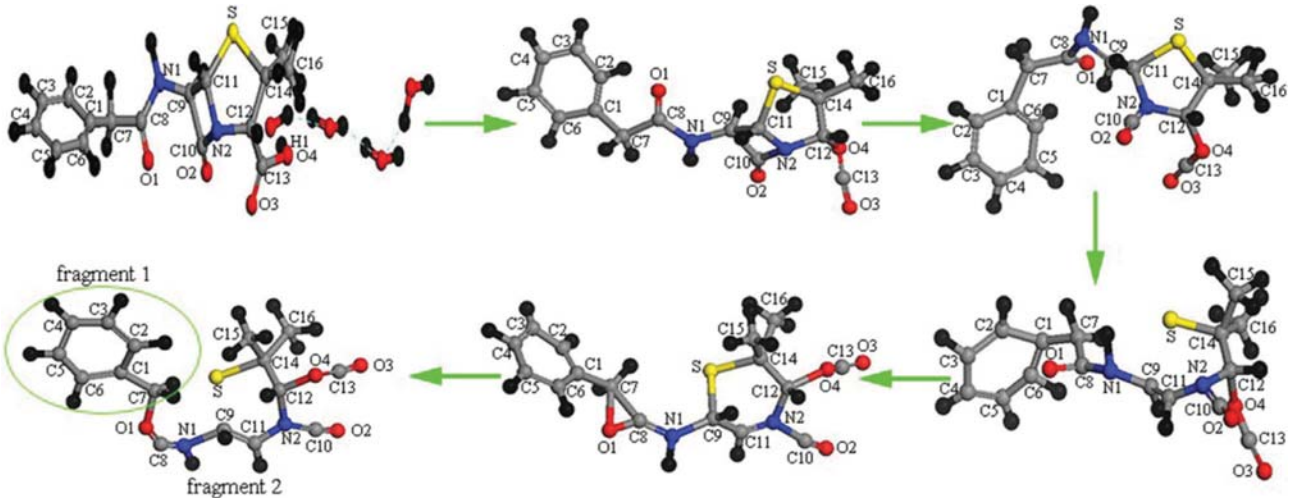

Fig. 9. Initial degradation of PCN in SCWO. The 2D degradation pathway was also displayed in Fig. S5 in the supporting information part.

cles were broken because of the structural instability. Then, the intermediate underwent intramolecular rearrangement by S atom interacting with C9 and linking with it, which caused O1 moving to the bridge site of C7 and C8. After that, the C7-C8 bond broke, and O1 inserted into the middle of C7 and C8, which was beneficial for the cleavage of linear chain (C7-O1 bond) and evolved PCN degraded into two small fragments, forming one aromatic ring (fragment 1) and one fragment containing N and S atoms (fragment 2). Moreover, degradation was initiated by the attack on O4 rather than the vulnerable β-lactam or thioether groups [47], indicating degradation of PCN was affected by steric hindrance, which is consistent with the experimental results.

2-3. Deeper Degradation of PCN During the SCWO Process

According to previous literature [48-50] and our experiment results, the formation of polycyclic aromatic hydrocarbons (PAHs) caused by polymerization among aromatic intermediates might retard the COD removal. In this regard, a deeper investigation on the decomposition of fragment 1 was essential, and the detailed degradation of fragment 1 is displayed in Fig. 10.

As seen, the aromatic ring was attacked by OH radical combined with O_2, the interaction of oxygen in the water cluster with the carbon atom in the ring induced one OH radical to dissociate from the water cluster, resulting in the formation of a chemical bond between C4 and O5. Then, an oxygen molecule interacted with C4 and captured H atom from it, forming an HO_2 radical. Subsequently, another oxygen molecule abstracted hydrogen from the hydroxyl group, only leaving O5 atom on the fragment 1. After that, another OH radical attacked C5 forming a chemical bond between C5 and O6. Besides, the H atom linked with C5 was captured by a hydroxyl radical forming a water molecule, and the intermediate underwent H migration from O6 to O5. Shortly afterward, an oxygen molecule moved towards fragment 1 and then interacted and connected with C2. As simulation continued, O6 moved to the bridge site of C4 and C5, and then the C4-C5 bond was broken, which caused O6 to be inserted into the aromatic ring. After that, the O5 lost its hydrogen under the action of HO_2 radical, and O=O bond was broken leaving O7 atom on the fragment. Finally, the oxygen atom from O_2 was embedded in the aromatic ring. The O atoms embedded in the aromatic ring can accelerate the aromatic ring opening for the reason that the C-O bond in the produced ring structure is much weaker than the C-C bond [25]. Consequently, the C2-O7 bond was broken and a linear chain with

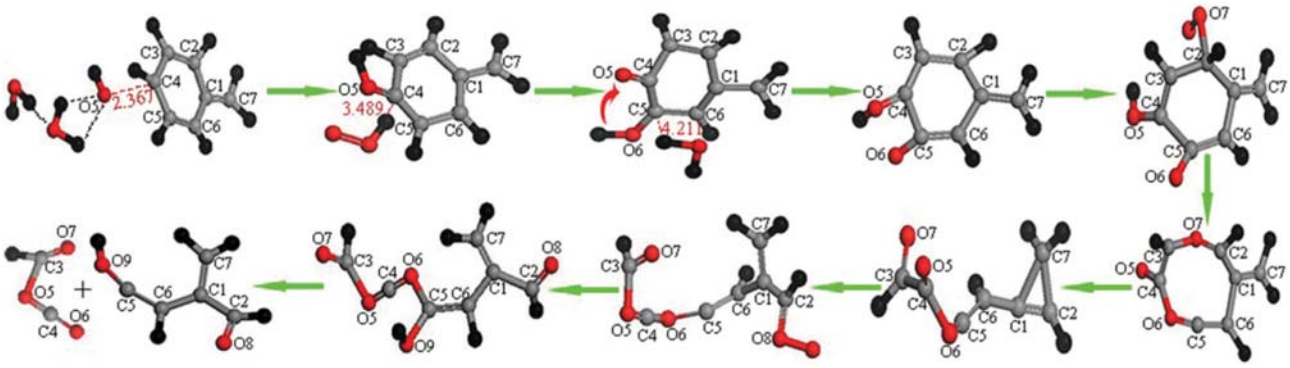

Fig. 10. The process of aromatic ring-opening reaction in SCWO. The 2D degradation pathway was also displayed in Fig. S6 in the supporting information part.

the three-membered ring formed. Under the attack of an oxygen molecule, the three-membered ring was opened through C2-C7 bond broken. The pathway attacked by O_2 was one of the main pathways for ring-opening reaction in SCWO [46]. Then, an OH radical further attacked C5 to reduce the C5-O6 bond strength, which was finally broken. After that, two smaller linear chains formed, and they further degraded into CO_2 and H_2O under the attack of OH radicals and O_2.

Previous studies [24,51] reported the ability of SCW to weaken C-C and C-heteroatom bonds, which may be partly responsible for the rapid ring-opening and chain cleavage reactions in SCW. Beyond that, benefitting from the less steric hindrance, the possibility of an attack by active radicals significantly improved. As a result, the cooperative effects between OH radicals and O_2 accelerated the ring-opening reaction by hydrogen abstraction and embedding O atoms into fragments, which would reduce the stability of the intermediate structure. Furthermore, incorporation of O atoms into alkane fragments may indicate that the SCW and oxidant acted as O sources for CO_2.

Fragment 2 was far from the stable structure. Therefore, intramolecular rearrangement took place by forming a chemical bond between C11 and S, which reduced the strength of C11-N2 bond and let it break. The hydrogen atoms in water cluster have been reported to interact with the heteroatoms in intermediates to promote the cleavage of most C-heteroatom bonds [24]. In this way, the water cluster served as both catalyst and reactant in the degradation process. For example, under the action of the water cluster, the C14-S bond was broken and fragment 2 degraded into two fragments (fragment 2a and 2b), which further interacted with OH radicals and oxygen molecules and degraded into more smaller fragments, as shown in Fig. 11.

For example, an OH radical moved towards fragment 2a and interacted with C11. Finally, a chemical bond between C11 and O10 formed, which reduced the strength of the C9=C11 bond, making it transform to a single bond. Then, the C9-N1 bond transformed to a double bond, which caused the breakage of the C8-N1 bond. The OH group linked with C11 also reduced the C11-S bond. Similar to C14-S bond cleavage, the C11-S bond was broken, which produced two fragments containing S atom and N atom, respectively. For fragment 2b, the C12-O4 bond was broken under the action of water cluster, resulting in C13 going away from fragment 2b in the form of CO_2 molecule. Subsequently, an oxygen molecule captured a hydrogen atom from N2, then the C16 provided its H atom to N2 and the C12-C16 bond formed, which reduced the strength of C12-N2 bond. Finally, C12-N2 bond was broken and two more smaller fragments formed. Like the aromatic ring, the fragment containing a three-membered ring was also attacked by OH radical combined with O_2.

2-4. Migration of S and N During the SCWO Process

Due to the tremendous harm to the environment and human health, migration of S and N is a crucial issue. Numerous studies [25,50,52-54] have reported the transformations of S and N in SCWO, but the routes and end products were variable. To understand how S and N transformed in SCWO, the routes for S and N transformation are described in Fig. 12.

Further analysis showed that S atom was transformed into H_2S under the action of OH radicals, HO_2 radicals, water cluster and H_2O_2 molecules. For S-containing fragment (Fig. 12(a)), an H_2O molecule provided hydrogen atom for S. Then, an OH radical interacted and connected with C8. Subsequently, another OH radical abstracted hydrogen from the hydroxyl group, which produced a water molecule. Under the action of the water cluster, the C8-S bond was broken, and a water molecule moved towards S-containing intermediate, which abstracted a hydrogen atom from the water molecule. Finally, an H_2S was produced. This hydrogen abstraction reaction suggested that SCW also played roles of H sources for H_2S. Green et al. [52] reported the decomposition of hexyl sulfide, and H_2S was found to be the main sulfur-contain-

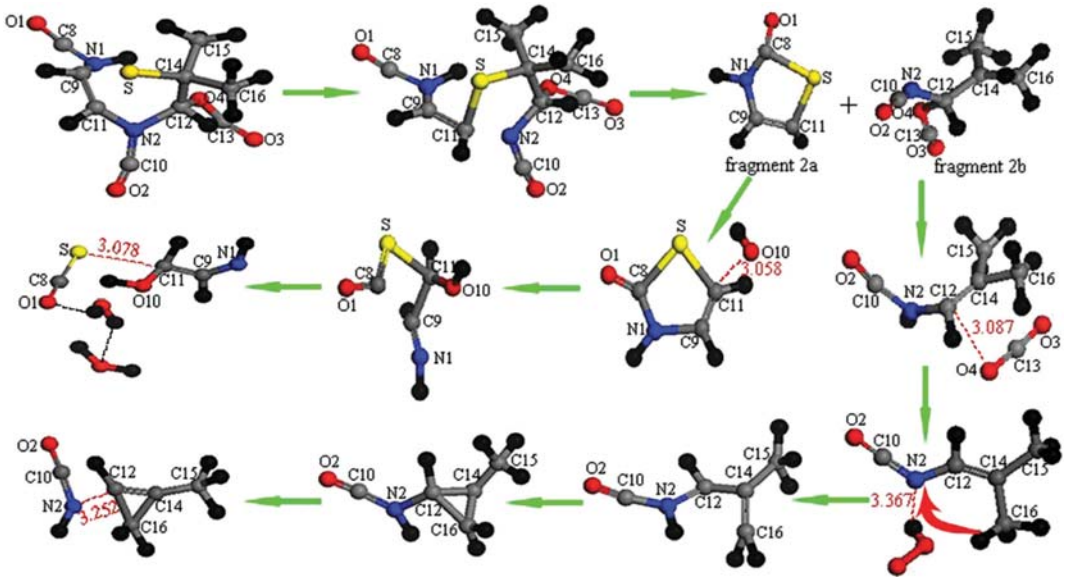

Fig. 11. The degradation process of fragment 2 in SCWO. The 2D degradation pathway was also displayed in Fig. S7 in the supporting information part.

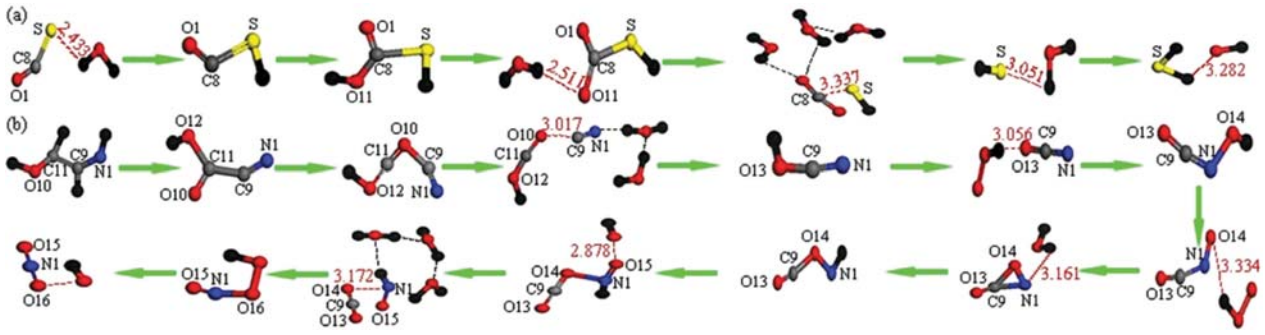

Fig. 12. The transformation of sulfur (a) and nitrogen (b) in SCWO. The 2D degradation pathway was also displayed in Fig. S8 in the supporting information part.

ing products. Moreover, they proposed a detailed pathway of the H_2S formation where SCW acted as not only the H sources but also an H-transfer catalyst.

For the N-containing fragments, they could transform into N_2 and oxynitride. Our simulation results showed that the N elements mainly transformed into NO_2 when the simulated SCWO system only included one PCN molecule (shown in Fig. 12(b)). In such a system, the number of N-containing fragments is very low. Thus, the collision probability between two N atoms was much smaller than that between N and O atoms, causing N elements to be transformed into NO_2 rather than N_2. Actually, by tracing the evolution of N elements with time, we observed that O atoms in NO_2 originated from SCW and oxidant, indicating a deep oxidation promoted by the reaction system.

CONCLUSIONS

The SCWO of penicillin was investigated in a batch reactor by varying process parameters. Experimental results showed that further increase of temperature contributed little to COD removal. Similar to the temperature, COD removal had no significant dependence on the pressure variations, owing to the two well-matched effects. Moreover, COD removal can be remarkably improved in the OC range of 0-2.0. Nevertheless, the effect was negligible as the OC value was greater than 2.0. Prolonging reaction time seemed to be less conducive to COD removal according to our experimental results.

Based on the ReaxFF molecular dynamics simulation, the degradation mechanism of PCN in SCWO system was obtained. By tracing the transformations of S and N in SCWO, migration routes were eventually established with H_2S, and NO_2 produced as the end products, respectively. Simulation results showed that in addition to the roles of producing reactive radicals and molecules, SCW and oxidant also acted as H sources for H_2S as well as O sources for CO_2 and NO_2. Catalysis of water clusters in C-heteroatom bond cleavage was also observed during the simulation process. In this way, the degradation process in SCWO system was greatly accelerated.

ACKNOWLEDGEMENTS

This work was supported by the National Natural Science Foundation of China (Grant Nos. 21576205) and the Program for Changjiang Scholars, Innovative Research Team in University (IRT_15R46).

NOMENCLATURE

$COD_{initial}$: initial COD content in the sample [mg L^{-1}]
COD_{final} : residual COD content in the liquid product [mg L^{-1}]
$[O_2]_{add}$: oxygen formed from the decomposition of H_2O_2 [mg]
$[O_2]_{need}$: stoichiometric oxygen needed to completely oxidize penicillin to CO_2, H_2O, SO_2 and NO_2 [mg]

SUPPORTING INFORMATION

Additional information as noted in the text. This information is available via the Internet at http://www.springer.com/chemistry/journal/11814.

REFERENCES

1. I. Michael, L. Rizzo, C. S. McArdell, C. M. Manaia, C. Merli, T. Schwartz, C. Dagot and D. Fatta-Kassinos, *Water Res.*, **47**, 957 (2013).
2. J. L. Martinez, *Environ. Pollut.*, **157**, 2893 (2009).
3. K. Kümmerer, *Chemosphere*, **75**, 417 (2009).
4. C. Ding and J. He, *Appl. Microbiol. Biotechnol.*, **87**, 925 (2010).
5. J. M. Cha, S. Yang and K. H. Carlson, *J. Chromatogr. A.*, **1115**, 46 (2006).
6. J. Altmann, A. S. Ruhl, F. Zietzschmann and M. Jekel, *Water Res.*, **55**, 185 (2014).
7. H. R. Pouretedal and N. Sadegh, *J. Water Process Eng.*, **1**, 64 (2014).
8. E. A. Serna-Galvis, J. Silva-Agredo, A. L. Giraldo-Aguirre, O. A. Flórez-Acosta and R. A. Torres-Palma, *Ultrason. Sonochem.*, **31**, 276 (2016).
9. A. L. Giraldo-Aguirre, E. D. Erazo-Erazo, O. A. Flórez-Acosta, E. A. Serna-Galvis and R. A. Torres-Palma, *J. Photochem. Photobiol., A.*, **311**, 95 (2015).
10. W. H. Glaze, J.-W. Kang and D. H. Chapin, *Ozone Sci. Eng.*, **9**, 335 (1987).
11. E. A. Serna-Galvis, J. Silva-Agredo, A. L. Giraldo, O. A. Flórez-Acosta and R. A. Torres-Palma, *Sci. Total Environ.*, **541**, 1431 (2016).
12. P. Villegas-Guzman, J. Silva-Agredo, O. Florez, A. L. Giraldo-Aguirre, C. Pulgarin and R. A. Torres-Palma, *J. Environ. Manage.*, **190**, 72 (2017).
13. L. Qian, S. Wang, D. Xu, Y. Guo, X. Tang and L. Wang, *Water Res.*,

89, 118 (2016).
14. O. Ö. Söğüt and M. Akgün, *J. Chem. Technol. Biotechnol.*, **85**, 640 (2010).
15. V. Vadillo, M. B. García-Jarana, J. Sánchez-Oneto, J. R. Portela and E. J. M. de la Ossa, *J. Chem. Technol. Biotechnol.*, **86**, 1049 (2011).
16. A. Loppinet-Serani, C. Aymonierand F. Cansell, *J. Chem. Technol. Biotechnol.*, **85**, 583 (2010).
17. B. Kayan and B. Gözmen, *J. Hazard. Mater.*, **201**, 100 (2012).
18. M. M. Islam, C. Zou, A. C. T. van Duin and S. Raman, *Phys. Chem. Chem. Phys.*, **18**, 761 (2016).
19. H. Takahashi, S. Hisaoka and T. Nitta, *Chem. Phys. Lett.*, **363**, 80 (2002).
20. Y. Zhang, J. Zhang, L. Zhao and C. Sheng, *Energy Fuels*, **24**, 95 (2010).
21. T. Honma and H. Inomata, *J. Supercrit. Fluids*, **90**, 1 (2014).
22. A. C. T. van Duin, S. Dasgupta, F. Lorant and W. A. Goddard, *J. Phys. Chem. A.*, **105**, 9396 (2001).
23. Y. Han, D. Jiang, J. Zhang, W. Li, Z. Gan and J. Gu, *FRONT. Chem. Sci. Eng.*, **1**, 16 (2016).
24. J. Zhang, X. Weng, Y. Han, W. Li, J. Cheng, Z. Gan and J. Gu, *Fuel*, **108**, 682 (2013).
25. J. Zhang, J. Gu, Y. Han, W. Li, Z. Gan and J. Gu, *Ind. Eng. Chem. Res.*, **54**, 1251 (2015).
26. J. Zhang, J. Gu, Y. Han, W. Li, Z. Gan and J. Gu, *J. Mol. Model.*, **21**, 54 (2015).
27. D. Jiang, Y. Wang, M. Zhang, J. Zhang, W. Li and Y. Han, *Int. J. Hydrogen Energy*, **15**, 9667 (2017).
28. E. Yabalak, H. A. Döndaş and A. M. Gizir, *J. Environ. Sci. Health, Part A.*, **3**, 210 (2017).
29. E. Salmon, A. C. T. van Duin, F. Lorant, P.-M. Marquaire and W. A. Goddard III, *Org. Geochem.*, **40**, 1195 (2009).
30. B. Chen, X.-Y. Wei, Z.-S. Yang, C. Liu, X. Fan, Y. Qing and Z.-M. Zong, *Energy Fuels*, **26**, 984 (2012).
31. H. Wang, H. A. G. Stern, D. Chakraborty, H. Bai, V. DiFilippo, J. S. Goela, M. A. Pickering and J. D. Gale, *Ind. Eng. Chem. Res.*, **52**, 15270 (2013).
32. P. E. Savage, *Chem. Rev.*, **99**, 603 (1999).
33. S. Wang, Y. Guo, L. Wang, Y. Wang, D. Xu and H. Ma, *Fuel Process. Technol.*, **92**, 291 (2011).
34. S. Gopalan and P. E. Savage, *AIChE J.*, **41**, 1864 (1995).
35. K. Minok, W. K. Lee and C. H. Lee, *Chem. Eng. Sci.*, **52**, 1201 (1997).
36. L. Li, P. Chen and E. F. Gloyna, *AIChE J.*, **37**, 1687 (1991).
37. D.-S. Lee, E. F. Gloyna and L. Li, *J. Supercrit. Fluids*, **3**, 249 (1990).
38. N. Segond, Y. Matsumura and K. Yamamoto, *Ind. Eng. Chem. Res.*, **41**, 6020 (2002).
39. N. Akiya and P. E. Savage, *Chem. Rev.*, **102**, 2725 (2002).
40. W.-J. Gong, F. Li and D.-L. Xi, *Water Environ. Res.*, **80**, 186 (2008).
41. S. Gopalan and P. E. Savage, *AIChE J.*, **41**, 1864 (1995).
42. J. L. DiNaro, J. W. Tester, J. B. Howard and K. C. Swallow, *AIChE J.*, **46**, 2274 (2000).
43. S. F. Rice and E. Croiset, *Ind. Eng. Chem. Res.*, **40**, 86 (2001).
44. P. E. Savage, J. Yu, N. Stylski and E. E. Brock, *J. Supercrit. Fluids*, **12**, 141 (1998).
45. H. Ma and J. Ma, *J. Chem. Phys.*, **135**, 054504 (2011).
46. J. Zhang, X. Weng, Y. Han, W. Li, Z. Gan and J. Gu, *J. Energy Chem.*, **22**, 459 (2013).
47. E. A. Serna-Galvis, J. Silva-Agredo, A. L. Giraldo, O. A. Flórez and R. A. Torres-Palma, *Chem. Eng. J.*, **284**, 953 (2016).
48. B. Shukla, A. Susa, A. Miyoshi and M. Koshi, *J. Phys. Chem. A.*, **112**, 2362 (2008).
49. A. Comandini, T. Malewicki and K. Brezinsky, *J. Phys. Chem. A.*, **116**, 2409 (2012).
50. Y. Gong, Y. Guo, S. Wang and W. Song, *Water Res.*, **100**, 116 (2016).
51. T. Fujii, R. Hayashi, S.-i. Kawasaki, A. Suzuki and Y. Oshima, *J. Supercrit. Fluids*, **58**, 142 (2011).
52. Y. Kida, C. A. Class, A. J. Concepcion, M. T. Timko and W. H. Green, *Phys. Chem. Chem. Phys.*, **16**, 9220 (2014).
53. N. Meng, D. Jiang, Y. Liu, Z. Gao, Y. Cao, J. Zhang, J. Gu and Y. Han, *Fuel*, **186**, 394 (2016).
54. J. Wang, F. He, Y. Li and H. Sun, *RSC Adv.*, **6**, 93260 (2016).

Supporting Information

Treatment of penicillin with supercritical water oxidation: Experimental study of combined ReaxFF molecular dynamics

Tengzhou Ma[*], Tingting Hu[***], Dandan Jiang[*], Jinli Zhang[*], Wei Li[*], You Han[*,,†], and Banu Örmeci[***,†]**

*School of Chemical Engineering and Technology, Tianjin University, Tianjin 300072, China
**Tianjin Key Laboratory of Membrane Science and Desalination Technology, Tianjin University, Tianjin 300072, China
***Department of Civil and Environmental Engineering, Carleton University,
1125 Colonel by Drive, Ottawa, Ontario K1S5B6, Canada
(*Received 13 July 2017 • accepted 12 December 2017*)

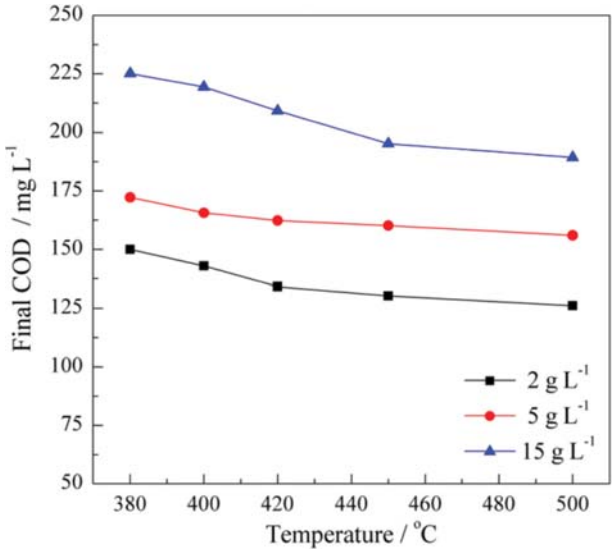

Fig. S1. Effect of temperature on final COD (pressure: 24 MPa; residence time: 1 min; OC: 2).

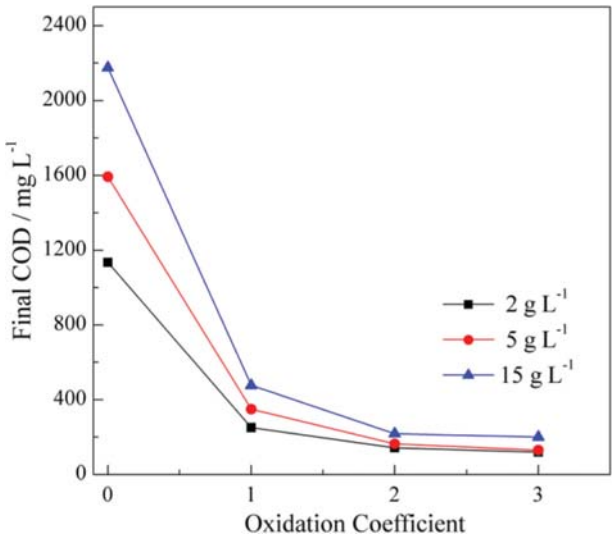

Fig. S3. Effect of oxidation coefficient on final COD (temperature: 400 °C; pressure: 24 MPa; residence time: 1 min).

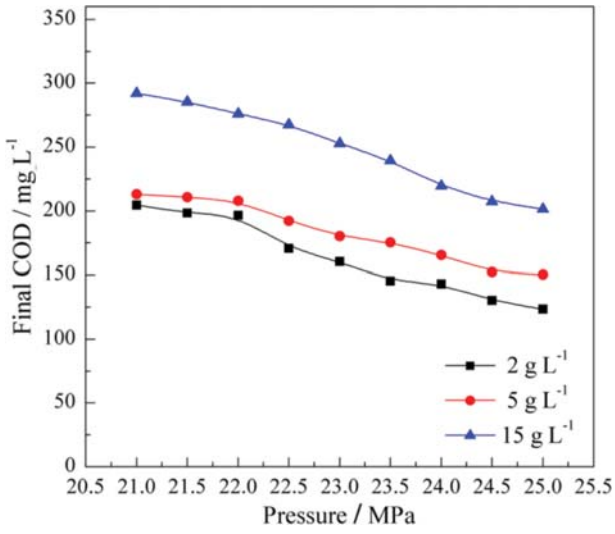

Fig. S2. Effect of pressure on final COD (temperature: 400 °C; residence time: 1 min; OC: 2).

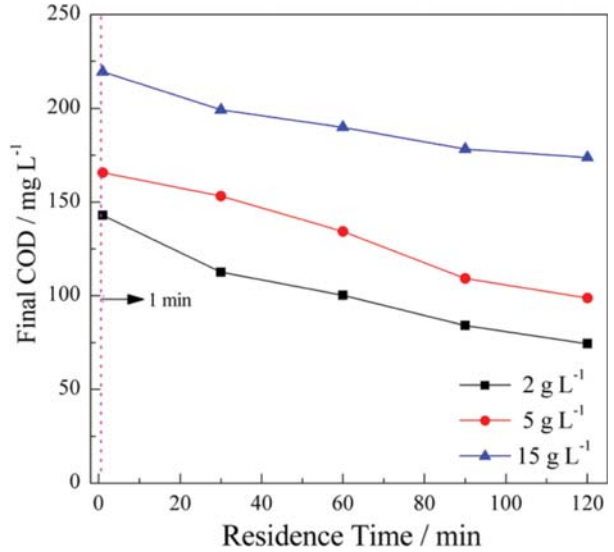

Fig. S4. Effect of residence time on final COD (temperature: 400 °C; pressure: 24 MPa; OC: 2).

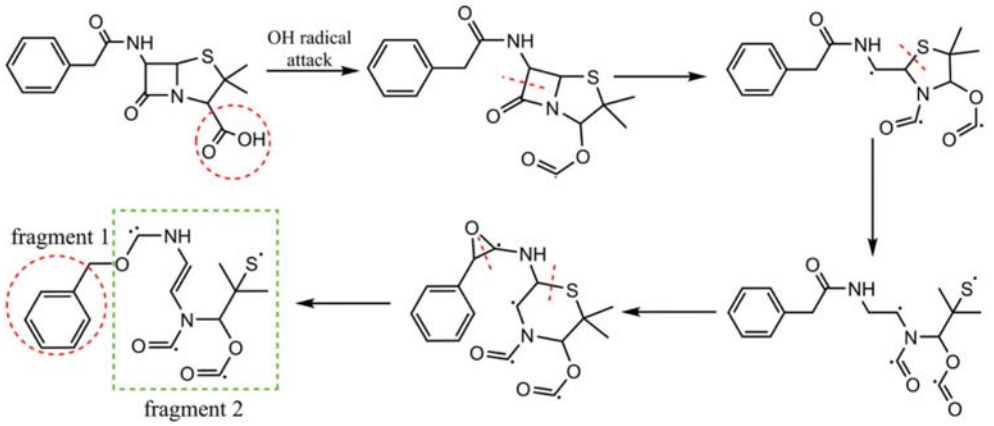

Fig. S5. Initial degradation of PCN in SCWO.

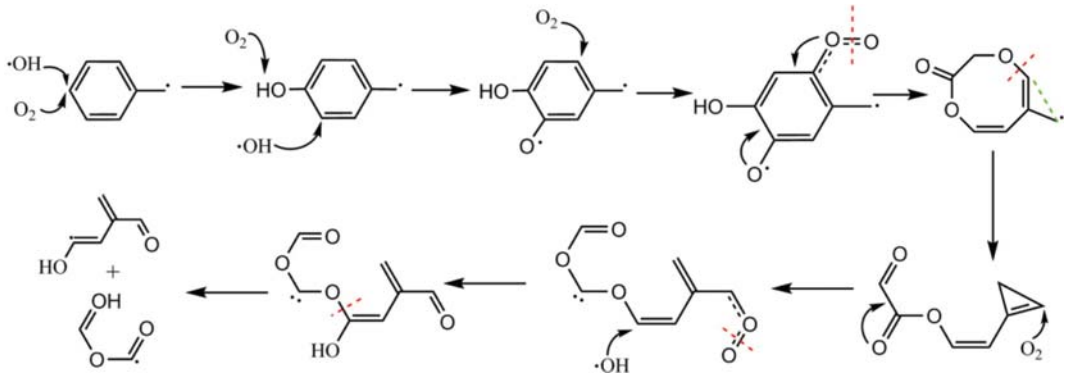

Fig. S6. The process of aromatic ring-opening reaction in SCWO.

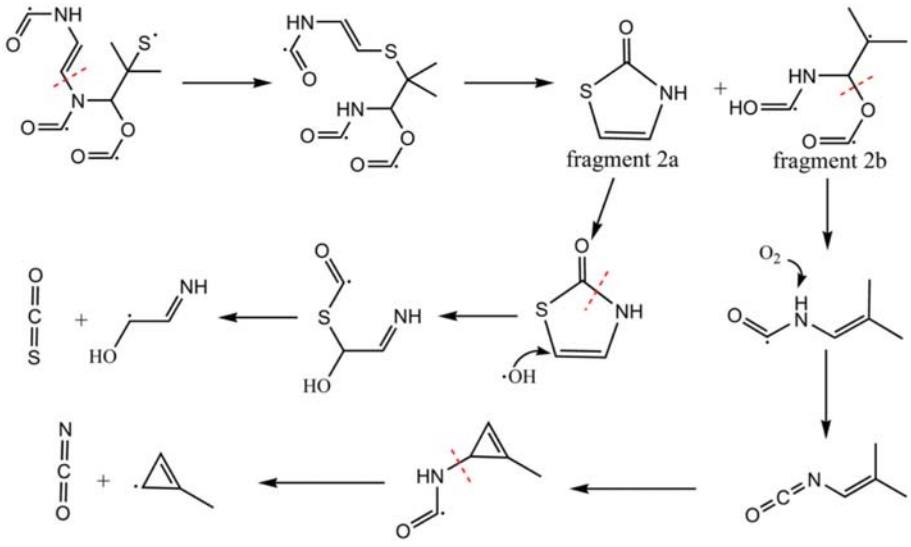

Fig. S7. The degradation process of fragment 2 in SCWO.

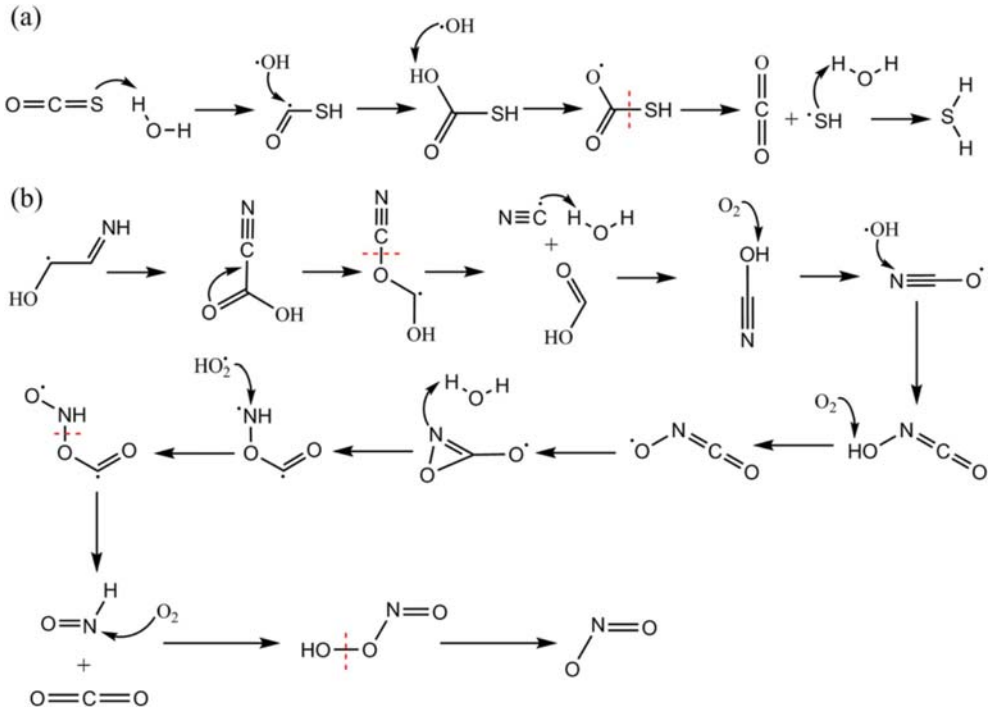

Fig. S8. The transformation of sulfur (a) and nitrogen (b) in SCWO.